Received: 17 June 2022 | Revised: 1 December 2022 | Accepted: 14 December 2022

IET Communications

DOI: 10.1049/cmu2.12560

The Institution of Engineering and Technology WILEY

ORIGINAL RESEARCH

Temporal prediction for spectrum environment maps with moving radiation sources

Yi Zhao[1] | Qiuming Zhu[1,2] | Zhipeng Lin[1] | Lantu Guo[3] | Qihui Wu[1] | Jie Wang[1] | Weizhi Zhong[1]

[1]The Key Laboratory of Dynamic Cognitive System of Electromagnetic Spectrum Space, Nanjing University of Aeronautics and Astronautics, Nanjing, China

[2]National Mobile Communications Research Laboratory, Southeast University, Nanjing, China

[3]China Research Institute of Radio Wave Propagation, Qingdao, China

Correspondence
Zhipeng Lin, The Key Laboratory of Dynamic Cognitive System of Electromagnetic Spectrum Space, Nanjing University of Aeronautics and Astronautics, Nanjing, China.
Email: linlzp@nuaa.edu.cn

Funding information
Key Technologies R&D Program of Jiangsu (Prospective and Key Technologies for Industry), Grant/Award Numbers: BE2022067, BE2022067-3; National Natural Science Foundation of China, Grant/Award Number: 62271250; Natural Science Foundation of Jiangsu Province, Grant/Award Number: BK20211182; National Key Scientific Instrument and Equipment Development Projects of China, Grant/Award Number: 61827801; Open Research Fund of National Mobile Communications Research Laboratory, Southeast University, Grant/Award Number: 2022D04; Basic Scientific Research Project, Grant/Award Number: NS2022046

Abstract

Spectrum resources are becoming harder to come by for wireless communications. The spectrum environment map (SEM), which depicts the electromagnetic environment's current state and future trend, is a valuable technique for managing and allocating spectrum resources. Most SEM construction approaches only take static SEMs into account and cannot forecast time-domain changes and trends of SEMs in dynamic scenes. In this paper, a brand-new temporal SEM prediction method for the high dynamic spectrum environment is proposed. This method is based on knowledge of radiation source and the optical flow driven by propagation channel models. First, a novel radiation source localization strategy is designed to obtain the radiation source movement information. Then, the optical flow field of the available SEMs is combined with the information regarding radiation source movement. In order to forecast future SEMs, a propagation model driven reconstruction technique is developed. Simulation findings demonstrate how well the suggested strategy is tailored to capture the spatiotemporal correlation of SEMs. This technique performs better than the state-of-the-art in terms of single- and multiple-step SEM predictions.

1 | INTRODUCTION

With the rapid development of wireless communications, the shortage of spectrum resources, the severity of spectrum security, and the intensity of spectrum confrontation are becoming increasingly severe [1–3]. As a new paradigm for the spectrum space, the radio environment map (REM) or the spectrum environment map (SEM) can visualize the current state and the future development trend of electromagnetic environments. Since electromagnetic radiation sources are often mobile in the realistic world, a dynamic SEM is vital to describe the realistic spectrum space. Temporal prediction is promising to obtain the dynamic SEM efficiently, since it can predict the unknown SEMs of the future based on the given current spectrum data. However, precise temporal prediction of dynamic spectrum spaces is challenging due to rapidly changing environments and complex electromagnetic propagation characteristics.

Many kinds of literatures addressed the problem of SEM prediction, but most only focused on the spatial prediction (or construction) of SEM. However, the SEM temporal prediction problem can be viewed as an image frame prediction problem. In that case, existing methods can be categorized into

three types, that is, centroid tracking method, cross-correlation method, and optical flow method. In radar echo prediction, the centroid tracking method can predict the global echo by extrapolating the position of the centroid [4]. Yet centroid extrapolation only conducts linear prediction, which is not effective in the complex electromagnetic environment. The cross-correlation method estimates the vector field of image motion change by correlation operation of previous frames of images, and then extrapolates subsequent frames based on frames of images and the field. For example, the authors in [5] took sub-regions of the image as the extrapolation target and make prediction for movements. Moreover, the optical flow vector field based method has been proven helpful in making accurate extrapolation of radar maps [6]. The optical flow field often has a global consistency. Thus, the optical flow filed is smoother than the field obtained by cross-correlation method. Note that, these methods only considered the correlation between image frames, while ignoring SEM's inherent electromagnetic propagation characteristics.

Recently, many researchers applied deep learning methods to deal with the sequence prediction [7–9]. Recurrent neural networks (RNNs) were widely used in video prediction and other areas [10–13]. For example, the authors in [14] constructed an RNN model to predict the subsequent frames for videos. In [15], the authors adapted the sequence to sequence long short-term memory (LSTM) framework for multiple frames prediction. These studies directly apply the sequence prediction methods to spatial-temporal prediction, ignoring the unique spatial characteristics. Furthermore, the authors in [16] extended the RNN model and proposed the convolutional LSTM (ConvLSTM) by plugging the convolutional operations into recurrent connections. By encoding spatial features with the convolutional operation, the LSTM and the convolutional neural network were effectively combined for the first time. In [17] and [18], the authors proposed and further improved a more complex spatiotemporal prediction framework called PredRNN. However, the deep learning methods for spatiotemporal prediction require long-term and large-scale datasets. For most applications, the spectrum monitoring equipment does not have a continuous long-term monitoring ability, and there is no large-scale historical dataset. Moreover, deep learning methods can not accurately model the rapidly changing characteristics of SEM in a time-varying environment.

In this paper, we propose a novel temporal prediction method for dynamic SEMs. A radiation source localization method is presented to extract the radiation source movement information. Then, the radiation source movement information and the optical flow field is merged to predict the future SEM by propagation model driven reconstruction method.

The main contributions of this paper are summarized as follows:

- By exploiting the spatiotemporal heterogeneity of SEMs, we propose a prediction method based on the radiation information and the optical flow. It can present the dynamic spectrum states under the scenario with moving radiation sources.
- We develop a radiation source localization method based on the persistent homology technology, which can be used to obtain the radiation source movement vectors.
- We develop an extrapolation method based on the propagation channel model. By considering the radio propagation characteristic, the radiation source movement vectors and optical flow field are combined to extrapolate the SEM.

The remainder of the article is organized as follows. In Section 2, we discuss the related works. Section 3 introduces time-variant SEM. Section 4 introduces the temporal prediction based on optical flow combined with radiation source movement information. The simulation results and analysis are provided in Section 5. The conclusions are drawn in Section 6.

2 | RELATED WORKS

Most existing studies focused on the construction (or prediction) of SEM in the space domain. They obtained the spectrum map by using the sparse sensor data to predict the missing data. For example, data-driven methods were usually used for the spatial prediction. These methods can be mainly classified into three major categories, that is, interpolation-based methods [19], tensor-based methods, and deep learning-based methods. The authors in [20] carried out a wide range of comparative studies on the interpolation-based SEM construction. The interpolation-based methods implicitly assume a static SEM of a particular frequency band, ignoring the fading phenomenon in electromagnetic propagation. The tensor-based methods employ tensor completion to predict SEM data. The author in [21] developed a joint tensor scheme to retrieve incomplete measurements. In [22], a 3D spectrum mapping framework, including spectrum situation estimation and spectrum recovery, was presented. Moreover, in [23], the optimization for sampling locations was utilized to improve the performance of SEM construction. By treating SEMs as images, deep learning methods are also introduced in the SEM construction. The authors in [24] developed a novel convolutional neural network structure for spectrum map construction. In [25], a deep network architecture was used to learn the propagation model from measured data. In [26], the authors proposed a deep neural network to estimate the path loss model in urban environments. The authors in [27] used an environment dependent channel model to construct the SEM. On the other hand, the model-driven methods are based on the radiation source information, propagation model or additional prior information. Although the accuracy of this kind of method is high, the number of reconstructed radiation sources is limited, and the reconstruction performance is dependent on the prior information [28, 29]. Recently, some researchers focused on the multi domain expansion of SEMs, but they were only concerned about the space-frequency domain [30, 31]. Despite significant efforts have been put into the SEM construction, it's infeasible to simply apply SEM construction methods to prediction in dynamically changing environments due to the inherent spatiotemporal heterogeneity.

TABLE 1 Related works on SEM construction

Method	Reference	Space domain	Frequency domain	Time domain
Interpolation	[19, 20]	✓	✗	✗
Tensor	[21–23]	✓	✗	✗
	[34, 35, 37]	✗	✓	✓
Deep learning	[24–27]	✓	✗	✗
	[30, 31]	✓	✓	✗
	[36]	✓	✗	✓
	[38]	✗	✓	✓
Hidden Markov model	[32]	✗	✗	✓
	[33]	✓	✗	✓
Propagation model	[28, 29]	✓	✗	✗
	Proposed method	✓	✗	✓

Different from the spatial prediction, the temporal prediction of SEM can forecast the unknown SEM by mining the change of historical observations. The authors in [32] used a Markov model to predict the time series of spectrum occupancy. This was a meaningful attempt to introduce the traditional time series prediction model into the spectrum prediction, but it only considered the time-varying characteristics of a single frequency band. In [33], spatial spectrum occupancy was predicted by a hidden Markov model, but only a single step prediction was made. Moreover, matrix or tensor-based methods are also proven useful in temporal prediction. In [34], the spectral-temporal prediction problem was transformed into a matrix recovery problem. In [35], a time-frequency-day spectrum tensor model was presented. Periodic characteristics among different days were further considered for the long-term prediction. In [36], the missing data from the spatial view was estimated in advance. Then, the authors conducted the prediction from the temporal view by using an RNN. This method is a two-step prediction method separating time and space dimensions. From the perspective of image inference, in [37, 38], SEM prediction was carried out in the time-frequency domain using tensor-based methods and deep learning, respectively. However, these methods both ignored the spatiotemporal need for prediction. The comparison of related works is summarized in Table 1.

3 | TIME-VARIANT SPECTRUM ENVIRONMENT

A realistic spectrum environment is complex and dynamic. The movement of radiation sources mainly causes time-varying characteristics in this environment. Locating mobile radiation sources and recognizing the time-varying multipath effect are two main problems in predicting time-varying spectrum environments. A typical time-variant spectrum environment in the suburban scenario is illustrated in Figure 1. Two vehicle radiation sources are moving. One fixed radiation source is placed on the top of the building. Firstly, the interested environment is gridded, and each grid is represented by the received signal strength (RSS) or other spectrum parameters. The SEM is composed of collected data at each instance is called a SEM frame. Due to the slow variation of the spectrum environment, we assume that the SEM frame is approximately fixed during a short time interval. The SEM frames are arranged in the time domain to form a time-variant SEM frame sequence, as shown in Figure 1. The spectrum data is usually collected by fixed monitoring nodes [39, 40] or moving monitoring nodes such as vehicles and unmanned aerial vehicles (UAVs). Since the collected data is sometimes limited, the proposed prediction method is used to predict the SEM frame of next time based on the previously observed SEM frames. Let us suppose an area represented by $M \times N$ grid, which consists of M rows and N columns. For each cell of the grid, the measured RSS data is time-variant. If we record T snapshots, it can be represented by a tensor $\mathbf{I}(x, y, t) \in \mathbf{R}^{M \times N \times T}$, where $\mathbf{R}$ denotes the domain of RSS. The temporal prediction of SEM can be expressed as

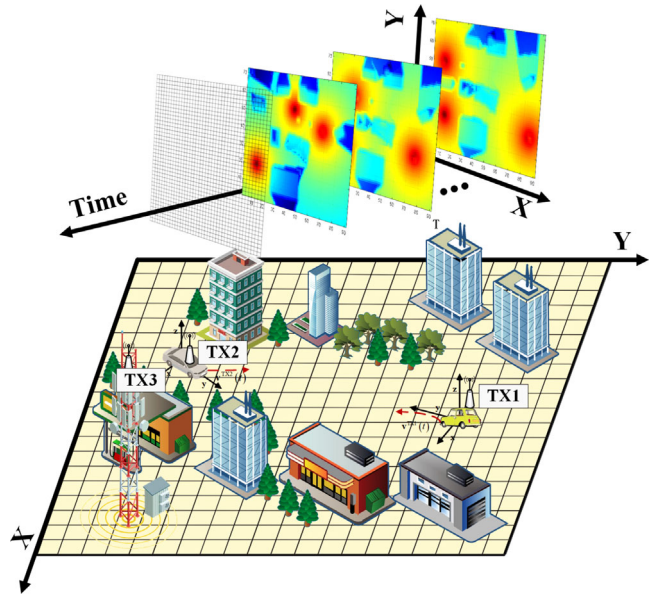

FIGURE 1 Time-variant spectrum environment with moving radiation sources

$$\mathbf{I}(t+1) = \underset{\mathbf{I}(t+1)}{\arg\max}\, p(\mathbf{I}(t+1)|\mathbf{I}(1)\cdots,\mathbf{I}(t-1),\mathbf{I}(t)), \quad (1)$$

where $\mathbf{I}(t)$ is the known RSS values or the SEM frame at t. For simplicity, this paper predicts the SEM only based on the last two frames, as given by

$$\mathbf{I}(t+1) = \underset{\mathbf{I}(t+1)}{\arg\max}\, p(\mathbf{I}(t+1)|\mathbf{I}(t-1),\mathbf{I}(t)). \quad (2)$$

4 | TEMPORAL PREDICTION WITH RADIATION INFORMATION AND OPTICAL FLOW

4.1 | An overview of prediction scheme

The locations of radiation sources in the measurement environment may change in time, and this variation changes the

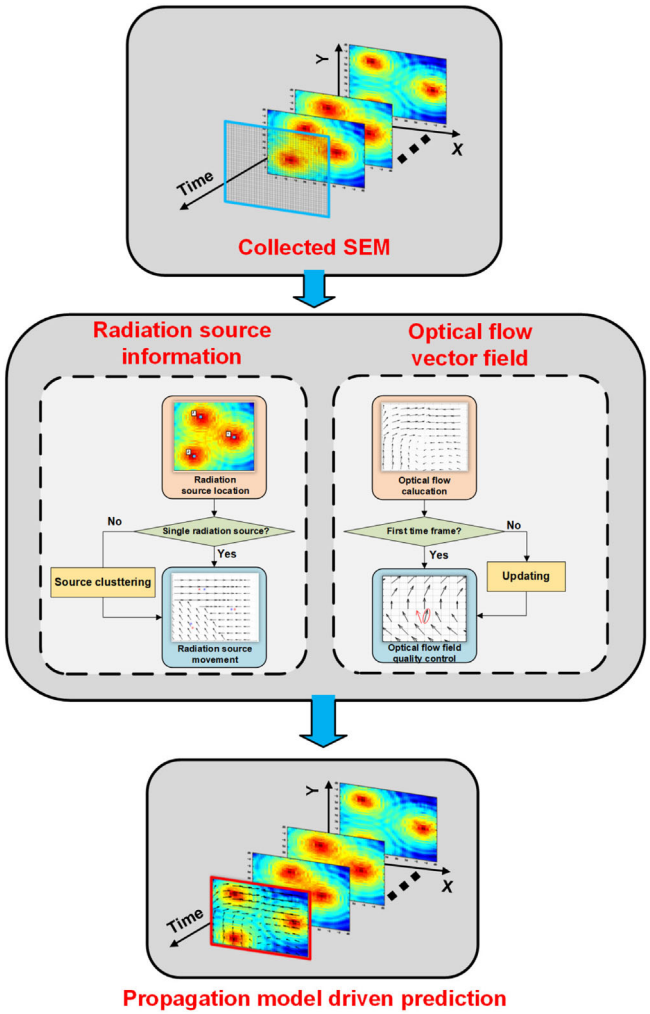

FIGURE 2 Flowchart of proposed SEM prediction scheme

ALGORITHM 1 Persistent homology based radiation source localization

Input: The SEM data frame $\mathbf{I}$.

Output: The position groups of radiation sources *Groups*.

Initialize the union-find instance uf and location position groups *Groups*.
Sort $\mathbf{I}$ in descending order.
for $j = 1; j <= sizeof(\mathbf{I}); j++$ **do**
  Initialize temp variable *temp*.
  repeat
    Search the neighbors of $\mathbf{I}_j$ by its coordinate index.
    if neighbors of $\mathbf{I}$ is in uf **then**
      $temp.append(\mathbf{I}_{j\_neighbor})$
    end if
  until All neighbors have been searched
  Sort *temp* in descending order.
  if j=1 **then**
    $Groups.append(\mathbf{I}_j)$
  end if
  $uf.append(\mathbf{I}_j)$
  $uf.union(\mathbf{I}_j, temp[0])$
  for $k = 2; k <=$ sizeof(*temp*); $k++$ **do**
    if *temp*[k] is not in *Groups* **then**
      $Groups.append(temp[k])$
    end if
    $uf.union(temp[0], temp[k])$
  end for
end for
return *Groups*

SEM in turn. In order to solve the problem of SEM prediction, we propose a scheme combining radiation source information extraction, the SEM optical flow vector field, and the propagation model driven prediction, as shown in Figure 2. Based on the collected previous SEM data, the radiation source motion vector field and optical flow vector field are calculated, respectively. If the number of radiation sources is more than one, a clustering method is used to group the radiation sources. Then, we perform the prediction based on the propagation model-driven method.

4.2 | Location and movement of radiation sources

Radiation source locations can be obtained in a SEM by searching the local peak of RSS values. In this paper, we use the persistent homology theory in topology to locate the radiation sources. Note that when the number of radiation sources exceeds 1, the radiation location clustering needs to be carried out.

We abstract these cells measured into points and triangulate the cells to obtain a complex S. The local peak in the SEM frame is a max value of a 0-th persistent homology group of S. To calculate 0-dimensional persistent homology, we use a union-find data structure. We arrange points in S in descending order and carry out neighborhood search for points. For points that have no searched points around, we create a new homology group and append the point to it. For points that have searched points around, we append the point to the group of searched points with the max value. The proposed method is summarized in Algorithm 1, and the persistent homology diagram is given in Figure 3.

This paper adopts a clustering algorithm to cluster and locate the radiation source. The number of clusters is equal to the number of located radiation sources. Since the prediction is in a short-term time interval, the radiation source can be grouped with the location of the last time. The motion vector of the radiation source can be calculated as

$$\mathbf{V}_k^t = \left(X_k^t - X_k^{t-1}, Y_k^t - Y_k^{t-1}\right), \tag{3}$$

where X_k^t is the x position of the k-th radiation source at time t, and Y_k^t is the y position of the k-th radiation source at time

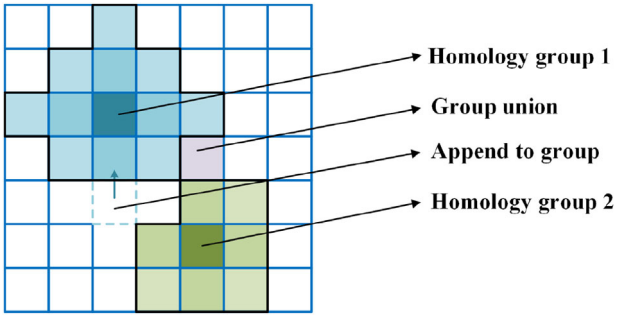

FIGURE 3 Persistent homology calculation diagram

t. Except that the motion vector information of the cell, where the radiation source is precisely located has been obtained. The motion vector information of other cells is determined by the motion vector of the nearest radiation source.

4.3 | Time-variant optical flow vector field

The optical flow refers to the instantaneous motion vector field in the image sequence due to the relative motion between the observed target and the observation area. The premise of the optical flow method is that the brightness between image frames is constant, which can be expressed as

$$I(x+u\Delta t, y+v\Delta t, t+\Delta t) = I(x,y,t), \tag{4}$$

where $I(x,y,t)$ is the value of point (x,y) at time t, u is the horizontal motion speed and v is the vertical motion speed.

Since the motion is always continuous, we can expand (4) by Taylor at point (x,y,t) and obtain

$$I(x,y,t) + \Delta x\frac{\partial I}{\partial x} + \Delta y\frac{\partial I}{\partial y} + \Delta t\frac{\partial I}{\partial t} + e = I(x,y,t), \tag{5}$$

where e is the higher order term of $\Delta x, \Delta y, \Delta t$. Furthermore, Equation (5) can be simplified as

$$\frac{\partial I}{\partial x}\frac{dx}{dt} + \frac{\partial I}{\partial y}\frac{dy}{dt} + \frac{\partial I}{\partial t} = 0. \tag{6}$$

For simplicity, we define

$$\begin{cases} I_x = \dfrac{\partial I}{\partial x}, \\ I_y = \dfrac{\partial I}{\partial y}, \\ I_t = \dfrac{\partial I}{\partial t}, \\ u = \dfrac{dx}{dt}, \\ v = \dfrac{dy}{dt}. \end{cases} \tag{7}$$

Then the optical flow constraint equation can be defined as

$$I_x u + I_y v + I_t = 0. \tag{8}$$

The key step of optical flow method is to solve (8) and obtain the optical flow vector field, that is, u and v. In order to explore the global change of SEM, we use an extended polynomial to estimate the background displacement [41]. This method does not require the spectrum space being stationary. The purpose of polynomial expansion is to approximate the neighborhood value of a pixel by using a polynomial, which is defined as

$$f(\mathbf{x})\ \mathbf{x}^T\mathbf{A}\mathbf{x} + \mathbf{b}^T\mathbf{x} + c, \tag{9}$$

where $\mathbf{A}$ is a symmetric matrix, $\mathbf{b}$ is a vector and c is a scalar. A weighted least mean square method is used to estimate the pixel value of the area around the pixel point, and thus, it can determine the coefficient of Equation (9). The result of polynomial expansion is to use a polynomial to estimate the adjacent region of pixels.The polynomial is analyzed in the case of ideal transformation, which is defined as

$$f_1(\mathbf{x})\ \mathbf{x}^T\mathbf{A}_1\mathbf{x} + \mathbf{b}_1{}^T\mathbf{x} + c_1. \tag{10}$$

A new signal f_2 is constructed by adding the global displacement $\mathbf{d}$ on the basis of the first frame signal data, which is expressed as

$$\begin{aligned} f_2(\mathbf{x}) &= f_1(\mathbf{x}-\mathbf{d}) \\ &= (\mathbf{x}-\mathbf{d})^T\mathbf{A}_1(\mathbf{x}-\mathbf{d}) + \mathbf{b}_1^T(\mathbf{x}-\mathbf{d}) + c_1 \\ &= \mathbf{x}^T\mathbf{A}_1\mathbf{x} + (\mathbf{b}_1 - 2\mathbf{A}_1\mathbf{d})^T\mathbf{x} + \mathbf{d}^T\mathbf{A}_1\mathbf{d} - \mathbf{b}_1^T\mathbf{d} + c_1. \\ &= \mathbf{x}^T\mathbf{A}_2\mathbf{x} + \mathbf{b}_2{}^T\mathbf{x} + c_2. \end{aligned} \tag{11}$$

Comparing (10) with (11), we have

$$\mathbf{A}_2 = \mathbf{A}_1, \tag{12}$$

$$\mathbf{b}_2 = \mathbf{b}_1 - 2\mathbf{A}_1\mathbf{d}, \tag{13}$$

$$c_2 = \mathbf{d}^T\mathbf{A}_1\mathbf{d} - \mathbf{b}_1^T\mathbf{d} + c_1. \tag{14}$$

if $\mathbf{A_1}$ is a nonsingular matrix, $\mathbf{d}$ can be obtained as

$$\mathbf{d} = -\frac{1}{2}\mathbf{A}_1^{-1}(\mathbf{b}_2 - \mathbf{b}_1), \tag{15}$$

where $\mathbf{d}$ is the global displacement between SEM frames. This method can reduce the iteration by a priori displacement value. An appropriate priori displacement value means smaller relative displacement, so it can accurately estimate the displacement between SEM frames. The best displacement between frames can also be obtained by iterative displacement estimation. The Farneback algorithm also generates a pyramid at multiple levels of resolution to solve an aperture problem, as shown in Figure 4. The Farneback method has good performance in global optical calculation. The average spatial angle error and the standard deviation are relatively small [42].

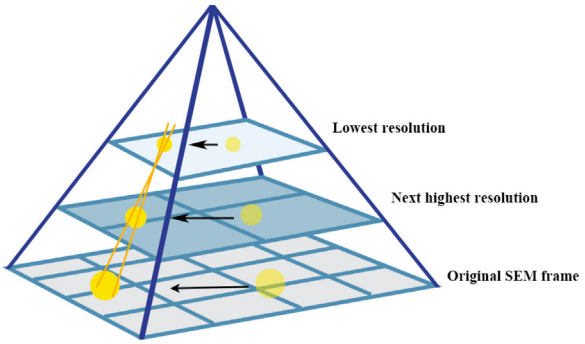

FIGURE 4 Optical flow calculation pyramid

4.4 | Propagation model driven prediction

After the values of the radiation source motion field and optical flow field are calculated, extrapolation prediction can be conducted. The extrapolation method is based on the assumption that the SEM motion remains unchanged in the short term. Since the actual SEM motion constantly changes, the extrapolation method has particular time effectiveness. In this paper, semi Lagrangian extrapolation is used for proximity prediction. Compared with linear extrapolation, semi Lagrangian extrapolation can be regarded as going up along the streamline to find the pixel moving to the current position, and thus, its prediction results are generally more accurate.

According to the displacement of points, we can obtain

$$\frac{I(x,y,T_0+\Delta t)-I(x-\alpha,y-\beta,T_0)}{\Delta t}=0, \tag{16}$$

where (x,y) represents the position to be predicted, T_0 is the current snapshot which is also the start time of prediction, Δt is the time interval of prediction, α is the displacement caused by the movement in the x direction within the predicted period, and β is the displacement caused by the movement in the y direction within the predicted period. Then $I(x,y,T_0+\Delta t)$ is expressed as the value of SEM data of cell (x,y) at $T_0+\Delta t$. Therefore, in order to predict, it is necessary to solve the motion displacement vector (α,β).

The semi Lagrangian extrapolation method is carried out in an iterative to solve (α,β). A n-order iterative displacement vector (α^n,β^n) is expressed as

$$\begin{cases}\alpha^n=\Delta t u\left(x-\dfrac{\alpha^{n-1}}{2},y-\dfrac{\beta^{n-1}}{2},T_0\right),\\ \beta^n=\Delta t v\left(x-\dfrac{\alpha^{n-1}}{2},y-\dfrac{\beta^{n-1}}{2},T_0\right).\end{cases} \tag{17}$$

It can be seen from Equations (16) and (17) that the position of the point extrapolated by semi Lagrangian is not always located exactly on the grid, interpolation is required to estimate the SEM data value at these locations. Therefore, selecting the appropriate interpolation method will affect the accuracy of calculation results and the effectiveness of prediction. Bilinear interpolation, cubic interpolation and other methods are usually used in the general optical flow prediction, and the classical IDW method is often used in the general SEM interpolation. However, these methods only consider the influence of distance. It assumes that the known sampling points near the unknown sampling points are more similar than those far away from the location while ignoring other factors, such as frequency that affect RSS in the real electromagnetic propagation environment. Considering the characteristics of the propagation environment, the weight of SEM prediction is path loss, not distance. Therefore, we use a method combined with a propagation model to interpolate and recover SEM data that is not precisely on the grid after optical flow prediction. The SEM values for unknown points can be obtained by

$$\hat{I}(x,y,T_0+\Delta t)=I(x-\alpha,y-\beta,T_0)=\sum_{i=1}^{R}\omega_i I(x_i,y_i,T_0), \tag{18}$$

where (x_i,y_i) are effective interpolation points, R is the total number of effective interpolation points, ω_i is interpolation coefficient, which can be calculated by

$$\omega_i=\frac{{L_i}^{-1}}{\sum_{k=1}^{R}{L_k}^{-1}}, \tag{19}$$

where L_i is the path loss between the position of $(x-\alpha,y-\beta)$ and effective interpolation points, which can be calculated by

$$L_i=32.45+20\lg(f)+20\lg(d_i), \tag{20}$$

where f is the center frequency of radiation source, d_i is the distance between point $(x-\alpha,y-\beta)$ and effective interpolation points.

5 | SIMULATION RESULTS AND ANALYSIS

5.1 | Experiment setup

In this section, simulations are conducted to demonstrate the effectiveness of the proposed SEM temporal prediction method. The experiment scenario is a campus soccer field of 100 m * 100 m. There are ten buildings with heights from 19 m to 35m around the field and the average height is about 20 m.

We use the ray tracing (RT) technique to obtain the SEM simulation results of this area. The RT technique is a widely used electromagnetic analysis method. The electromagnetic wave is viewed as a bunch of rays, so a geometric solution can be obtained based on uniform diffraction and geometric optics theory. After tracking all rays, a lot of propagation parameters can be obtained. In this article, we only concentrate on the received signal strength.

TABLE 2 Radiation source parameter

Index	Location (m)			Speed (m/s)			Frequency (GHz)	Bandwidth (MHz)	Antenna type	Transmitting power (dBm)
	x	y	z	x	y	z				
1	75	47.5	2	−5	0	0	1	10	Isotropic	0
2	22.5	20	2	0	5	0	1	10	Isotropic	0
3	32.5	77.5	2	5	0	0	1	10	Isotropic	0

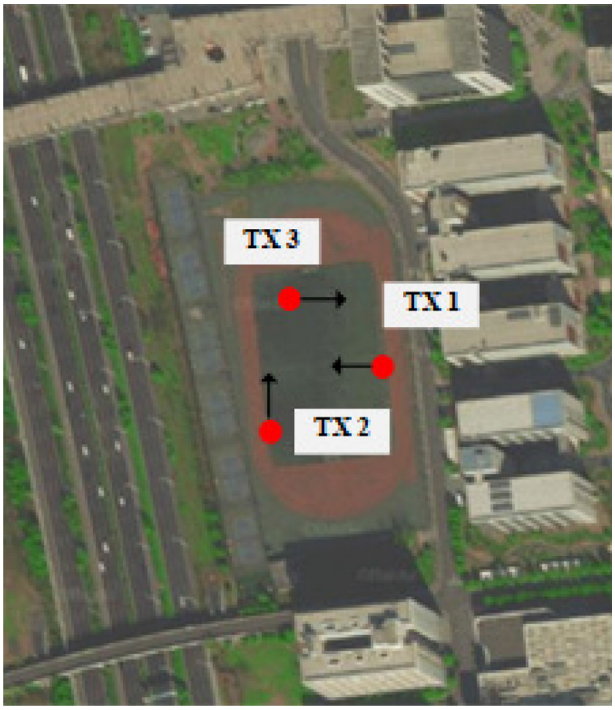

FIGURE 5 SEM Simulation scenario

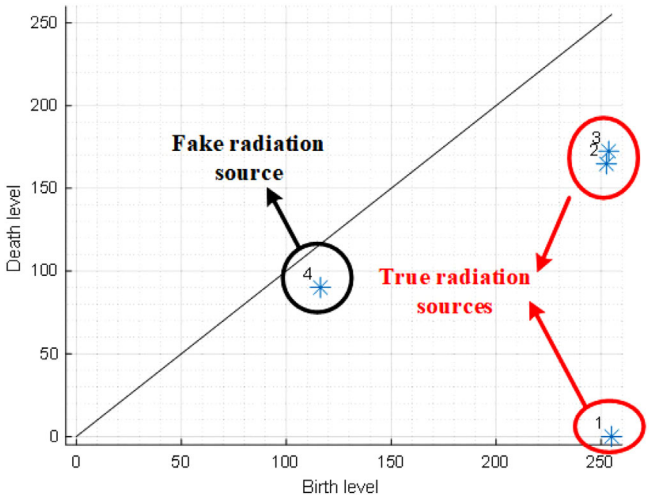

FIGURE 6 Localization persistence diagram at frame 1

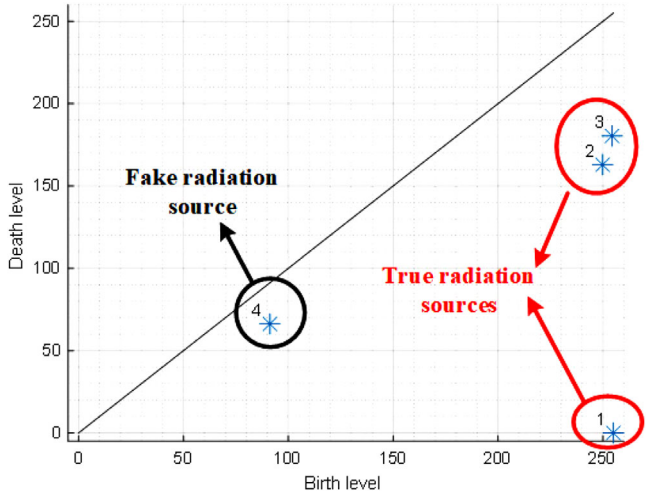

FIGURE 7 Localization persistence diagram at frame 2

Three mobile radiation sources are placed in the simulation scenario, as shown in Figure 5. They continuously transmit a single-tone signal with the power of 0 dBm at 1 GHz and move at the speed of 5 m/s. The detailed parameter information is shown in Table 2.

Since this is a dynamic scene with moving radiation sources, we consider six different timesteps and obtain six frames of the SEM. The first two frames of SEM are used as the input information of prediction, and the SEM of the last four frames is used as the ground truth to compare with the predicted SEMs.

5.2 | Localization and optical flow acquisition

Firstly, we calculate the 0-dimensional persistent homology problem to locate the radiation sources. We define the difference between birth level and death level as the persistence value. It is seen from Figures 6 and 7 that the homology class of the radiation source positions are concentrated on the right. In other words, the radiation source location points are homology classes with higher birth and lower death levels. Those homology classes closer to the line in the figure, such as class 4, are jumped values due to the phenomena of reflection and scattering in complex propagation scenes because of their small persistence value. Therefore, class 4 is a fake radiation source.The locations of the three radiation sources are shown in Figure 8, which conform to the assumption of local maxima. The radiation source moves slowly between frames.

Since the radiation source movement is a short-term change. We perform a clustering algorithm to gather the radiation

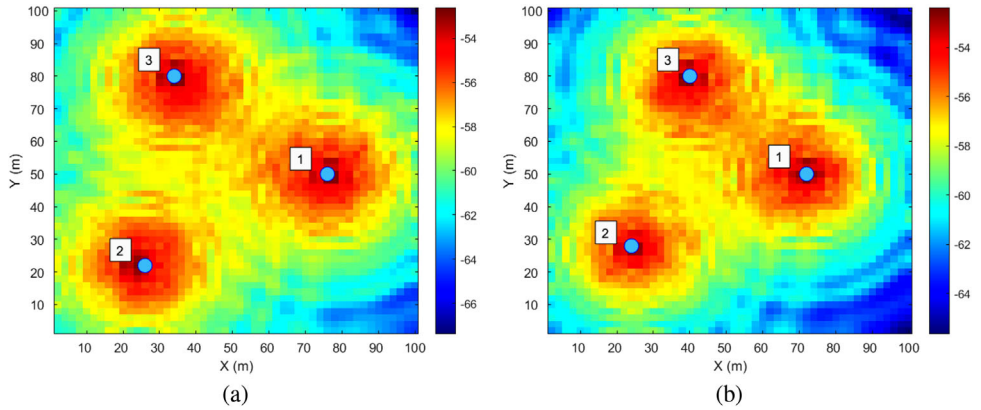

FIGURE 8 Radiation source locations: (a) radiation locations at frame 1; (b) radiation locations at frame 2

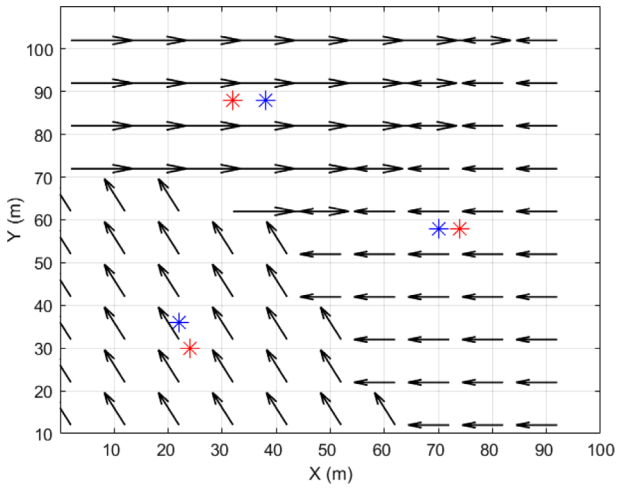

FIGURE 9 Radiation motion vector field

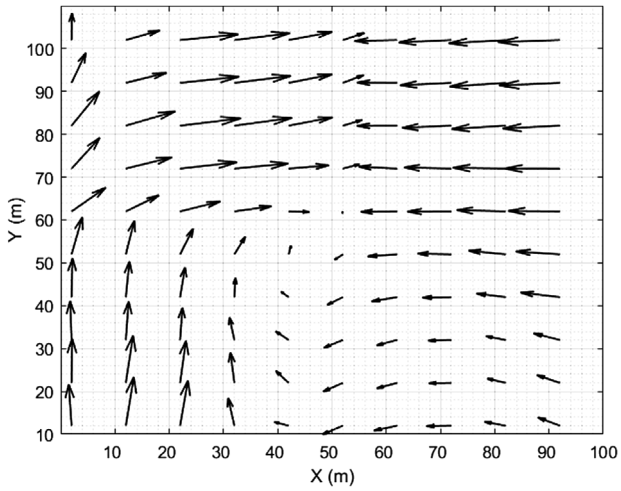

FIGURE 10 Optical flow vector field

sources closer between two SEM frames into a cluster. Then, we calculate the motion vector field, as shown in Figure 9. On the other hand, we calculate the optical flow and obtain the optical flow vector field, as shown in Figure 10.

It is described in Figures 9 and 10 that the motion vector field well shows the linear change of the radiation source positions according to the change of the position of different radiation sources. However, it does not reflect the transition between different movements. The optical flow vector field is based on the principle of brightness conservation, and the vector field changes smoothly. On the one hand, the overall change reflected is consistent with the motion vector field, on the other hand, there is a smooth connection between different motions. However, some vector values are small and have a weak impact on the change of SEM. Thus, we combine the motion vector field and the optical flow in the prediction.

5.3 | Prediction performance

Figure 11 shows the theoretical predicted SEM and the results of three different prediction methods. In Figure 11b, the prediction is made by the cross-correlation block matching method [5], which calculates the motion vector field between images by dividing images into blocks and matching them. It can be found that the predicted SEM image has prominent blocking characteristics. Moreover, the radiation source has an inevitable tear. Figure 11c is predicted by the basic optical flow method. Since the bilinear interpolation used in optical flow prediction introduces some outliers, quadratic interpolation is carried out. It can be found that there are certain cuts at the edge. In Figure 11d, the prediction is made by the model driven optical flow method assisted by the motion vector field of the radiation source. The overall prediction results are relatively smooth, and the characteristics of radiation sources are clear.

To compare the performance of the different prediction methods, we make a multi-step prediction and introduce root mean square error (RMSE) as the performance evaluation standard. The RMSE represents the error between the ground truth and the predicted value obtained by our method, which is defined as

$$RMSE = 10\log_{10}\frac{||\mathbf{I}(t) - \mathbf{I}(t)_{sim}||_2}{||\mathbf{I}(t)_{sim}||_2}, \tag{21}$$

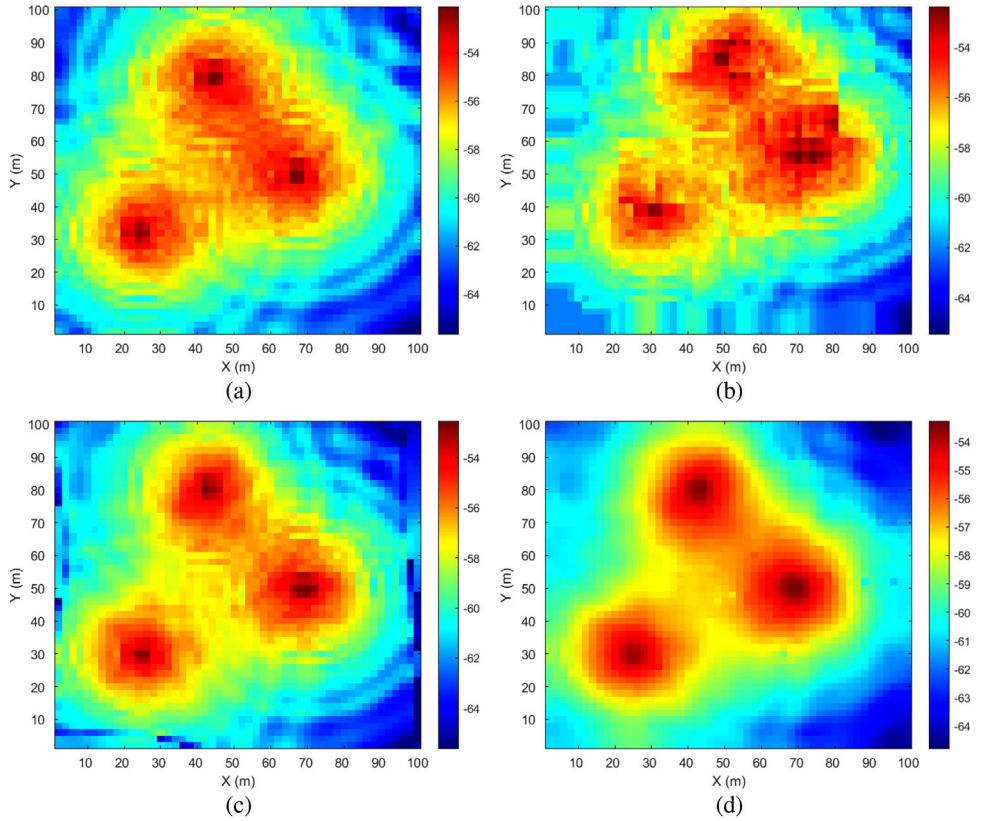

FIGURE 11 Predicted SEM: (a) theoretical SEM at frame 3; (b) cross correlation method; (c) optical flow method; (d) proposed method

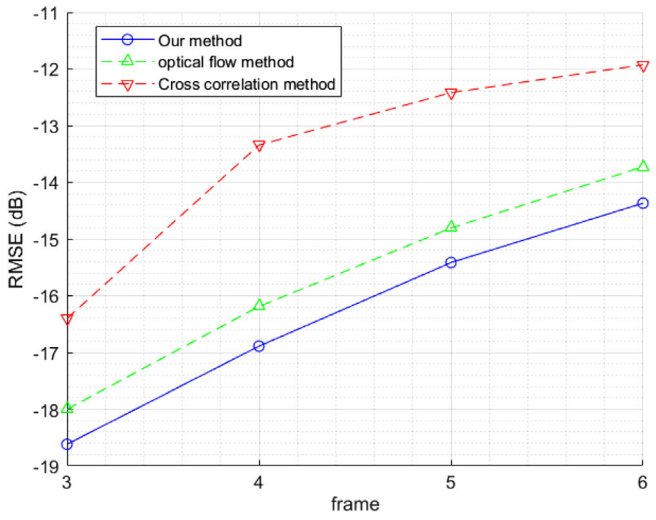

FIGURE 12 Comparison of RMSE by different methods

where $\mathbf{I}(t)$ is the predicted SEM, and $\mathbf{I}(t)_{sim}$ is the theoretical simulation SEM.

In Figure 12, the iterative prediction of 4-time steps is carried out. It can be found that the method proposed by this paper is better than the primary optical flow method and cross-correlation method. In addition, with the growth of prediction time steps, the RMSE of all prediction methods is rising. This is because, with the increase of time, the correlation between the SEM in the future and the existing SEM data is decreasing. The extrapolation through the current SEM data motion change field and optical flow field cannot make an accurate prediction.

6 | CONCLUSIONS

In this work, we have proposed a temporal SEM prediction method for time-varying spectrum environments. The extraction of radiation source location information and the acquisition of global constrained optical flow has been first conducted. Then, the radiation source movement vectors and optical flow vector field have been integrated, and the channel model driven extrapolation method has been used to predict the SEMs. It has shown that the proposed method is promising for performing precise SEM prediction in both single and multiple steps, according to experiments. The areas of precise SEM prediction in space-time-frequency domains and quick SEM temporal prediction in time-varying settings will be studied further.

AUTHOR CONTRIBUTIONS

Yi Zhao: Software, visualization, writing - original draft, writing - review and editing. Qiuming Zhu: Supervision, validation, writing - review and editing. Zhipeng Lin: Writing - review and editing. Lantu Guo: Supervision. Qihui Wu: Conceptualization, supervision. Jie Wang: Supervision, validation. Weizhi Zhong: Supervision.

ACKNOWLEDGEMENTS

This work was supported in part by the National Key Scientific Instrument and Equipment Development Project under Grant No. 61827801, in part by the National Natural Science Foundation of China under Grant No. 62271250, in part by Natural Science Foundation of Jiangsu Province, No. BK20211182 in part by the Key Technologies R&D Program of Jiangsu (Prospective and Key Technologies for Industry) under Grants BE2022067 and BE2022067-3, in part by the open research fund of National Mobile Communications Research Laboratory, Southeast University, No. 2022D04.

CONFLICT OF INTEREST

The authors declare no conflict of interest.

DATA AVAILABILITY STATEMENT

Research data are not shared.

ORCID

Qiuming Zhu https://orcid.org/0000-0002-4995-5970

REFERENCES

1. Tang, M., Zheng, Z., Ding, G., Xue, Z.: Efficient tv white space database construction via spectrum sensing and spatial inference. In: 2015 IEEE 34th International Performance Computing and Communications Conference (IPCCC), pp. 1–5. IEEE, Piscataway (2015)
2. Hanif, M.F., Smith, P.J., Dmochowski, P.A.: Statistical interference modelling and deployment issues for cognitive radio systems in shadow fading environments. IET Commun. 6(13), 1920–1929 (2012)
3. Elderini, T., Kaabouch, N., Reyes, H.: Channel quality estimation metrics in cognitive radio networks: a survey. IET Commun. 11(8), 1173–1179 (2017)
4. Johnson, J., MacKeen, P.L., Witt, A., Mitchell, E.D.W., Stumpf, G.J., Eilts, M.D., et al.: The storm cell identification and tracking algorithm: An enhanced wsr-88d algorithm. Weather Forecast. 13(2), 263–276 (1998)
5. Hamill, T.M., Nehrkorn, T.: A short-term cloud forecast scheme using cross correlations. Weather Forecast. 8(4), 401–411 (1993)
6. Sakaino, H.: Spatio-temporal image pattern prediction method based on a physical model with time-varying optical flow. IEEE Trans. Geosci. Remote Sens. 51(5), 3023–3036 (2012)
7. Hussain, W., Gao, H., Raza, M.R., Rabhi, F.A., Merigo, J.M.: Assessing cloud qos predictions using owa in neural network methods. Neural Comput. Appl. 34, 14895–14912 (2022)
8. Hussain, W., Merigó, J.M., Raza, M.R., Gao, H.: A new qos prediction model using hybrid iowa-anfis with fuzzy c-means, subtractive clustering and grid partitioning. Inf. Sci. 584, 280–300 (2022)
9. Hussain, W., Raza, M.R., Jan, M.A., Merigo, J.M., Gao, H.: Cloud risk management with owa-lstm predictive intelligence and fuzzy linguistic decision making. IEEE Trans. Fuzzy Syst. 30(11), 4657–4666 (2022)
10. Gao, H., Xiao, J., Yin, Y., Liu, T., Shi, J.: A mutually supervised graph attention network for few-shot segmentation: The perspective of fully utilizing limited samples. IEEE Trans. Neural Networks Learn. Syst. (2022)
11. Gao, H., Qiu, B., Barroso, R.J.D., Hussain, W., Xu, Y., Wang, X.: Tsmae: a novel anomaly detection approach for internet of things time series data using memory-augmented autoencoder. IEEE Trans. Network Sci. Eng. (2022)
12. Xu, Y., Wu, Y., Gao, H., Song, S., Yin, Y., Xiao, X.: Collaborative apis recommendation for artificial intelligence of things with information fusion. Future Gener. Comput. Syst. 125, 471–479 (2021)
13. Yin, Y., Huang, Q., Gao, H., Xu, Y.: Personalized apis recommendation with cognitive knowledge mining for industrial systems. IEEE Trans. Ind. Inf. 17(9), 6153–6161 (2020)
14. Donahue, J., Anne Hendricks, L., Guadarrama, S., Rohrbach, M., Venugopalan, S., Saenko, K., et al.: Long-term recurrent convolutional networks for visual recognition and description. In: Proceedings of the IEEE Conference on Computer Vision and Pattern Recognition, pp. 2625–2634. IEEE, Piscataway (2015)
15. Sutskever, I., Vinyals, O., Le, Q.V.: Sequence to sequence learning with neural networks. In: Advances in Neural Information Processing Systems, vol. 27. MIT Press, Cambridge, MA (2014)
16. Shi, X., Chen, Z., Wang, H., Yeung, D.Y., Wong, W.K., Woo, W.c.: Convolutional lstm network: A machine learning approach for precipitation nowcasting. In: Advances in Neural Information Processing Systems, vol. 28. MIT Press, Cambridge, MA (2015)
17. Wang, Y., Long, M., Wang, J., Gao, Z., Yu, P.S.: Predrnn: Recurrent neural networks for predictive learning using spatiotemporal lstms. In: Advances in Neural Information Processing Systems, vol. 30. MIT Press, Cambridge, MA (2017)
18. Wang, Y., Gao, Z., Long, M., Wang, J., Philip, S.Y.: Predrnn++: Towards a resolution of the deep-in-time dilemma in spatiotemporal predictive learning. In: International Conference on Machine Learning, pp. 5123–5132. International Machine Learning Society, Madison, WI (2018)
19. Debroy, S., Bhattacharjee, S., Chatterjee, M.: Spectrum map and its application in resource management in cognitive radio networks. IEEE Trans. Cognit. Commun. Netw. 1(4), 406–419 (2015)
20. Pesko, M., Javornik, T., Kosir, A., Stular, M., Mohorcic, M.: Radio environment maps: The survey of construction methods. KSII Trans. Internet Inf. Syst. (TIIS) 8(11), 3789–3809 (2014)
21. Tang, M., Ding, G., Wu, Q., Xue, Z., Tsiftsis, T.A.: A joint tensor completion and prediction scheme for multi-dimensional spectrum map construction. IEEE Access 4, 8044–8052 (2016)
22. Wu, Q., Shen, F., Wang, Z., Ding, G.: 3d spectrum mapping based on roi-driven uav deployment. IEEE Netw. 34(5), 24–31 (2020)
23. Shen, F., Wang, Z., Ding, G., Li, K., Wu, Q.: 3d compressed spectrum mapping with sampling locations optimization in spectrum-heterogeneous environment. IEEE Trans. Wireless Commun. 21(1), 326–338 (2021)
24. Hashimoto, R., Suto, K.: Sicnn: Spatial interpolation with convolutional neural networks for radio environment mapping. In: 2020 International Conference on Artificial Intelligence in Information and Communication (ICAIIC), pp. 167–170. IEEE, Piscataway (2020)
25. Teganya, Y., Romero, D.: Data-driven spectrum cartography via deep completion autoencoders. In: ICC 2020-2020 IEEE International Conference on Communications (ICC), pp. 1–7. IEEE, Piscataway (2020)
26. Levie, R., Yapar, Ç., Kutyniok, G., Caire, G.: Radiounet: Fast radio map estimation with convolutional neural networks. IEEE Trans. Wireless Commun. 20(6), 4001–4015 (2021)
27. Thrane, J., Zibar, D., Christiansen, H.L.: Model-aided deep learning method for path loss prediction in mobile communication systems at 2.6 Ghz. IEEE Access 8, 7925–7936 (2020)
28. Yilmaz, H.B., Tugcu, T.: Location estimation-based radio environment map construction in fading channels. Wireless Commun. Mobile Comput. 15(3), 561–570 (2015)
29. Sun, G., Van de Beek, J.: Simple distributed interference source localization for radio environment mapping. In: 2010 IFIP Wireless Days, pp. 1–5. IEEE, Piscataway (2010)
30. Sato, K., Inage, K., Fujii, T.: Radio environment map construction with joint space-frequency interpolation. In: 2020 International Conference on Artificial Intelligence in Information and Communication (ICAIIC), pp. 051–054. IEEE, Piscataway (2020)
31. Shrestha, S., Fu, X., Hong, M.: Deep generative model learning for blind spectrum cartography with nmf-based radio map disaggregation. In: ICASSP 2021-2021 IEEE International Conference on Acoustics, Speech and Signal Processing (ICASSP), pp. 4920–4924. IEEE, Piscataway (2021)
32. Eltom, H., Kandeepan, S., Moran, B., Evans, R.J.: Spectrum occupancy prediction using a hidden markov model. In: 2015 9th International Conference on Signal Processing and Communication Systems (ICSPCS), pp. 1–8. IEEE, Piscataway (2015)
33. Huang, L., Shao, W., Zhang, Y., Yang, J., Liu, Y.: A radio environment map construction scheme with hidden markov model based spectrum occupancy prediction. In: Proceedings of the 3rd International Conference

on High Performance Compilation, Computing and Communications, pp. 173–177. The Association for Computing Machinery, New York (2019)
34. Ding, G., Wu, F., Wu, Q., Tang, S., Song, F., Vasilakos, A.V., et al.: Robust online spectrum prediction with incomplete and corrupted historical observations. IEEE Trans. Veh. Technol. 66(9), 8022–8036 (2017)
35. Ge, C., Wang, Z., Zhang, X.: Robust long-term spectrum prediction with missing values and sparse anomalies. IEEE Access 7, 16655–16664 (2019)
36. Agarwal, A., Gangopadhyay, R.: Predictive spectrum occupancy probability-based spatio-temporal dynamic channel allocation map for future cognitive wireless networks. Trans. Emerg. Telecommun. Technol. 29(8), e3442 (2018)
37. Sun, J., Wang, J., Ding, G., Shen, L., Yang, J., Wu, Q., et al.: Long-term spectrum state prediction: An image inference perspective. IEEE Access 6, 43489–43498 (2018)
38. Yu, L., Chen, J., Ding, G.: Spectrum prediction via long short term memory. In: 2017 3rd IEEE International Conference on Computer and Communications (ICCC), pp. 643–647. IEEE, Piscataway (2017)
39. Ezzati, N., Taheri, H., Tugcu, T.: Optimised sensor network for transmitter localisation and radio environment mapping. IET Commun. 10(16), 2170–2178 (2016)
40. Kolakowski, M.: Automatic radio map creation in a fingerprinting-based ble/uwb localisation system. IET Microwaves Antennas Propag. 14(14), 1758–1765 (2020)
41. Farnebäck, G.: Two-frame motion estimation based on polynomial expansion. In: Scandinavian Conference on Image Analysis, pp. 363–370. Springer, Cham (2003)
42. Sun, H., Yan, L., Mooney, P., Liang, R.: A new method for moving object detection using variable resolution bionic compound eyes. Int. J. Phys. Sci. 6(24), 5618–5622 (2011)

How to cite this article: Zhao, Y., Zhu, Q., Lin, Z., Guo, L., Wu, Q., Wang, J., Zhong, W.: Temporal prediction for spectrum environment maps with moving radiation sources. IET Commun. 17, 538–548 (2023). https://doi.org/10.1049/cmu2.12560